Journal of Infection xxx (xxxx) xxx

Contents lists available at ScienceDirect

Journal of Infection

journal homepage: www.elsevier.com/locate/jinf

# Downregulation of *IGF2* expression in third trimester placental tissues from Zika virus infected women in Brazil

Andréia A. Suzukawa[a,1], Camila Zanluca[a,1], Natasha A.N. Jorge[b,1], Lucia de Noronha[c,1], Andrea C. Koishi[a], Caroline B.V. de Paula[c], Patrícia Z. Rebutini[c], Seigo Nagashima[c], Aruana F.F. Hansel-Frose[d], Vinícius S.C. Parreira[d], Juliano Bordignon[a], Margaret R. MacDonald[e], Charles M. Rice[e], Fabio Passetti[d,*], Claudia Nunes Duarte dos Santos[a,*]

[a] *Laboratório de Virologia Molecular, Instituto Carlos Chagas, Fundação Oswaldo Cruz, Curitiba, PR, Brazil*
[b] *Bioinformatics Group, Department of Computer Science, and Interdisciplinary Center for Bioinformatics, D-04107 Leipzig, Germany*
[c] *Laboratório de Patologia Experimental, Pontifícia Universidade Católica do Paraná, Curitiba, PR, Brazil*
[d] *Laboratório de Regulação da Expressão Gênica, Instituto Carlos Chagas, Fundação Oswaldo Cruz, Curitiba, PR, Brazil*
[e] *Laboratory of Virology and Infectious Disease, The Rockefeller University, New York, NY 10065, USA*

ARTICLE INFO

*Article history:*
Accepted 23 September 2020
Available online xxx

*Keywords:*
Zika virus
Placenta
Transcriptome
Insulin-Like Growth Factor II
Decidua

SUMMARY

*Objectives:* Screening for genes differentially expressed in placental tissues, aiming to identify transcriptional signatures that may be involved in ZIKV congenital pathogenesis.
*Methods:* Transcriptome data from placental tissues of pregnant women naturally infected with Zika virus during the third trimester were compared to those from women who tested negative for Zika infection. The findings were validated using both a cell culture model and an immunohistochemistry/morphological analysis of naturally infected placental tissues.
*Results:* Transcriptome analysis revealed that Zika virus infection induces downregulation of insulin-like growth factor II (*IGF2*) gene, an essential factor for fetal development. The Caco-2 cell culture model that constitutively expresses *IGF2* was used for the transcriptome validation. Asiatic and African Zika virus strains infection caused downregulated *IGF2* gene expression in Caco-2 cells, whereas other flaviviruses, such as dengue serotype 1, West Nile and wild-type yellow fever viruses, had no effect on this gene expression. Immunohistochemical assays on decidual tissues corroborated our transcriptome analysis, showing that IGF2 is reduced in the decidua of Zika virus-infected women.
*Conclusions:* Our results draw attention to *IGF2* modulation in uterine tissues, and this finding is expected to support future studies on strategies to ameliorate the harmful effects of Zika virus infection during pregnancy.



## Introduction

Zika virus (ZIKV) is an emerging arbovirus belonging to the genus *Flavivirus*, family *Flaviviridae*, which includes other viruses relevant to public health, such as dengue (DENV), yellow fever (YFV) and West Nile (WNV) viruses. Although ZIKV infection in humans is often characterized as a self-limiting disease,[1,2] infections during pregnancy can lead to fetal malformations and neurodevelopment abnormalities.[3–5]

A major worldwide effort is underway to shed light on different aspects of ZIKV infection in humans; however, the mechanisms by which ZIKV is transmitted to intrauterine tissues, the target cell types it affects and its effects on placental tissues are not completely clear.

By the study from mice and monkeys cells and tissues and from human *ex vivo* models, significant progress has been made in the characterization of genes differentially regulated during ZIKV infection, highlighting the host response to infection during pregnancy, which mainly involves the immune and inflammatory pathways.[6–9]

* Corresponding authors.
*E-mail addresses:* fabio.passetti@fiocruz.br (F. Passetti), claudia.dossantos@fiocruz.br (C.N. Duarte dos Santos).
[1] AAS, CZ, NANJ, and LN contributed equally to this work.

https://doi.org/10.1016/j.jinf.2020.09.028

Although the information obtained from these studies is relevant and helps to advance knowledge on ZIKV-induced congenitally abnormal outcomes, many of these studies were performed under controlled conditions, and the overall context of a natural infection route cannot be reproduced.

Here, the transcriptome profile of placental tissues from pregnant women naturally infected with ZIKV during the third trimester of gestation were compared to placental tissues with no evidence of ZIKV infection. Despite the intrinsic genetic differences and the restricted panel of samples, we were able to identify more than a thousand differentially expressed genes in the ZIKV-positive placenta tissues. The transcriptome analysis showed a significant decrease in the gene expression of insulin-like growth factor II (*IGF2*) in the placental tissues from women with a confirmed ZIKV diagnosis.

Hormones, growth factors and nutrients in the maternal and fetal circulation regulate placental development. The insulin/insulin-like growth factor (IGF) system, which comprises the peptide hormones insulin, IGF1, IGF2, and IGF-binding proteins, is implicated in the tight regulation of fetal and placental growth.[10] In this context, IGF2 plays a fundamental role in fetal development, and its dysfunctional expression results in abnormal congenital outcomes.[11]

In recent years, substantial knowledge has been accumulated on ZIKV infection during pregnancy. Nevertheless, only a few articles using naturally infected human tissues have been published. To our knowledge, this is the first report of a placental transcriptome analysis of women infected by ZIKV at late stages of pregnancy.

In view of the severity of ZIKV infection during gestation, understanding of the host response to this infection through the analyses of gene modulation may open new avenues for Zika therapy, clinical management, and vaccine development.

## Material and methods

### *Human samples and Ethics Approval*

This study was approved by Fiocruz and the Brazilian National Ethics Committee of Human Experimentation under the number CAAE: 42481115.7.0000.5248 and was carried out in compliance with ethical principles. The waiver for written informed consent was obtained when the Molecular Virology Laboratory was identified as a Reference Center for the Diagnosis of Emerging Viruses by the Brazilian Ministry of Health.

Human placenta samples from ZIKV-infected pregnant women during the third trimester of gestation and women not infected with ZIKV (hereafter referred to as non-ZIKV) were obtained immediately after delivery. Fragments comprising both fetal and maternal tissues were kept frozen (without preservatives) for molecular purposes. Tissue sections were also formalin-fixed/paraffin embedded for further anatomopathological, morphometric and immunohistochemical analyses. ZIKV infection was confirmed either during the acute phase of disease or after delivery by molecular or immunohistochemical techniques. All the tests were performed in laboratories of the Brazilian public health network. Detailed clinical characterization of the ZIKV positive case series, including pathological and laboratory findings, had been previously described.[12] Briefly, all women included as ZIKV positive cases (LRV/16 284, LRV/16 848, LRV/16 854, LRV/16 859, LRV/16 927, and LRV/16 931) were likely infected during the 7$^{th}$ or 8$^{th}$ gestational month and delivered at term. No congenital disorder was observed at birth, and the placentas were either normal or showed mild pathological changes. Placentas comprised in non-ZIKV group (LRV/16 986, LRV/16 1094, LRV/16 1098, LRV/16 1121, LRV/16 1220, LRV/16 1387; LRV/18 560, and LRV/18 563) were those from patients who were either not suspected of infection or tested negative for ZIKV. All but one (LRV/16 1387) non-ZIKV placentas were delivered at term.

### *RNA-Seq and transcriptome data analysis*

Total RNA from tissues was obtained following the manufacturer's instructions using an RNeasy kit (Qiagen, Hilden, Germany) with modifications. Briefly, 30 mg of tissue was disrupted in tubes with 5 mm metal beads under low temperature using two 2-minute cycles with 30 oscillations/minute in a TissueLyser LT (Qiagen) instrument. Tissue powder was resuspended in RTL buffer containing 10 µl/ml $\beta$-mercaptoethanol. A TRIzol reagent (Life Technologies, Rockville, MD) method was used and chloroform extraction performed prior to RNA purification using an RNeasy mini kit per the instruction manual. The quality and yield of the RNA samples were determined on a bioanalyzer platform using a total RNA nanoassay for eukaryotes (Agilent Technologies, Santa Clara, USA). Transcriptome libraries were prepared using the TruSeq Stranded Total RNA LT kit with Ribo-zero (Illumina, San Diego, USA). The 12 libraries were pooled together and sequenced in one lane of high-output 75 paired-end reads on an Illumina Next-Seq 500 sequencer.

The sequenced reads were aligned against the human genome GRCh37 sequence from Ensembl using HISAT2 version 2.1.0, retaining only the uniquely aligned reads (N:H:1 SAM flag) (parameters –dta, –fr, -q, –no-mixed, and –no-discordant). HTSeq version 0.10.0 with GENCODE (version 19) annotations of the human genome transcriptome was used to identify the expressed genes and infer the number of reads aligned to each gene (parameters: -t exon, -m intersection-nonempty, -r name, -i gene_id, and -s reverse). All statistical analyses were performed in R statistical software version 3.4.4 with DESeq2 version 1.18.1 and pheatmap version 1.0.12. The raw gene expression counts and DESeq2 were used to obtain the CPM values. Genes presenting a CPM count less than 20 in three or fewer samples were considered to be unexpressed and were removed from the analysis. We compared the normalized counts following the DESeq2 standard protocol and considered all genes presenting the $\log_2$ fold change (logFC) module $\geq$ 1.5 and an adjusted p-value $\leq$ 0.05 as differentially expressed. The differentially expressed genes (adjusted p-value $\leq$ 0.05) were used as input for the Bioconductor gage version 2.36 package.[13,14] This package selects up- and downregulated genes on which to perform 2 gene set enrichment analyses using the KEGG database. Pathways presenting the adjusted p-value $\leq$ 0.05 were considered statistically significant.

### *Cell culture model for transcriptome validation*

Caco-2 cells (ATCC HTB-37TM *Homo sapiens* colon colorectal cells), which tested negative for mycoplasma contamination (MycoAlert® Mycoplasma Detection kit, Lonza, Basel, Switzerland), were seeded in 6-well plates at a confluency of 5.0 x $10^5$ cells per well. After incubation overnight at 37°C and 5% $CO_2$, the cells were infected with Asian-lineage ZIKV (ZV BR 2015/15261 or ZV BR 2016/16288), which had been recently isolated from clinical specimens,[15] or with the African strain ZIKV MR766 at an MOI of 1. For comparative purposes, the Caco-2 cells were either uninfected (a mock control) or infected with a DENV-1 LRV/13400 isolate, WNV E/7229/06, wild-type YFV M17/09[16] or YFV strain used for vaccines (the 17DD strain) at the same MOI. All viruses were diluted in DMEM-F12 supplemented with 100 IU/µg/mL penicillin/streptomycin for inoculation. After 90 minutes, the inocula were removed, and the monolayers were washed three times with PBS (Lonza, Basel, Switzerland). The cells were maintained in DMEM-F12 containing 10% FBS and penicillin/streptomycin at 100

Please cite this article as: A.A. Suzukawa, C. Zanluca, N.A.N. Jorge et al., Downregulation of IGF2 expression in third trimester placental tissues from Zika virus infected women in Brazil, Journal of Infection, https://doi.org/10.1016/j.jinf.2020.09.028

IU/µg/mL (all reagents were obtained from Thermo Fischer Scientific, Grand Island, USA). At 24, 48 and 72 h post infection (h.p.i.), the cells were harvested for RNA extraction using an RNeasy Mini kit (Qiagen) following the manufacturer's instructions. RNA was quantified using a NanoDrop system (Thermo Scientific, Waltham, Massachusetts, United States), and the concentration was normalized to 8 ng/µL in nuclease-free water.

The expression of the *IGF2* gene was assessed by real-time RT-PCR as follows: Primers and probes (Table S1) were synthesized by Integrated DNA Technologies (IDT, Coralville, USA). The *IGF2* and *RNase P* genes were assessed using a TaqMan system, while a SYBR Green assay was used to quantify endogenous SDHA and YWHAZ genes. The reactions were standardized to range from 90 to 110% efficiency. All real-time assays were performed with one-step reaction systems (Promega, Madison, Wisconsin, United States) in the QuantStudio 5 instrument (Applied Biosystem, Foster City, California, United States). The stability of endogenous genes was evaluated by the GeNorm program and resulted in an M-factor lower than 0.37 for all time points. Gene expression analysis was performed according to the double delta CT method,[17] taking individual efficiencies into account. Statistical analysis was performed in Prism software (GraphPad version 6, USA) using two-way ANOVA followed by Tukey's test. Values of $p < 0.05$ indicated significance. Real-time RT-PCR was also used to assess intracellular viral RNA, as published elsewhere (protocols are indicated in the Table S1).

### *Viral titration and immunofluorescence*

To evaluate viable viral particles, supernatants of flavivirus-infected Caco-2 cells were titrated in ten-fold serial dilutions for a focus-forming assay using a C6/36 cell monolayer and were overlaid with a mixture of carboxymethylcellulose (1.6%), Leibovitz's L-15 medium, 0.26% tryptose and 5% FBS. After 7 days, the cells were fixed with 3% paraformaldehyde and then incubated with the anti-flavivirus monoclonal antibody 4G2 (hybridoma D1-4G2-4-15, ATCC HB-112) followed by anti-mouse IgG alkaline phosphatase-conjugated antibody (Catalog S372B - Promega, Madison, Wisconsin, United States). The reactions were developed with 5-bromo-4-chloro-3-indolyl-phosphate/nitro blue tetrazolium (BCIP/NBT) color development substrate (Promega).

Viral infection was also analyzed by indirect immunofluorescence. Cells were infected as described above. Cells were fixed with a methanol:acetone 1:1 solution 24, 48 and 72 h.p.i. The cells were then stained with 4G2 followed by goat anti-mouse IgG Alexa Fluor 488-conjugated antibody (Catalog A11001 - Life Technologies, Carlsbad, California, United States), and cell nuclei were counterstained with DAPI. Images were obtained with an Operetta high-content imaging system (PerkinElmer, Waltham, Massachusetts, United States) with a 20× objective and analyzed with Harmony High-Content Imaging and Analysis Software according to a previously established setup.[18]

Statistical analysis was performed in Prism software (GraphPad version 6, USA) using two-way ANOVA followed by Tukey's test. Values of $p < 0.05$ indicated significance.

### *Immunohistochemistry, semiquantitative analysis and statistics*

IGF2 expression in placentas was evaluated by immunohistochemistry in all the cases, however, because of improper fixation (autolysis) or unavailability of suitable tissue sections, some samples (LRV/16 986; LRV/16 1098 and LRV/16 1094) were inappropriate for accurate analysis. Then, 4-$\mu$m histological sections from six ZIKV-positive (LRV/16 284, LRV/16 848, LRV/16 854, LRV/16 859, LRV/16 927, and LRV/16 931) and four non-ZIKV (LRV/18 560; LRV/18 563; LRV/16 1220; LRV/16 1387) samples were subjected to immunohistochemistry. Slides were subjected to deparaffinization, dehydration, and rehydration. Endogenous peroxidase was blocked with methyl alcohol and hydrogen peroxide (the first block) followed by distilled water and hydrogen peroxide (the second block). Antigen retrieval was performed using a Bio SB$^{TM}$ ImmunoDNA Retriever. Slides were incubated overnight with the primary antibodies (anti-IGF2 rabbit polyclonal antibody, Catalog ab9574 – Abcam, Cambridge, UK) in a humid chamber from 2 to 8°C. Next, the slides were incubated with a secondary polymer (Reveal Polyvalent HRP-DAB Detection System – Spring Bioscience, Pleasanton, USA) for 25 minutes at room temperature. The reaction was developed with 3,3'-diaminobenzidine (DAB) in the presence of a hydrogen peroxide substrate for 3 minutes followed by counterstaining with Harris hematoxylin. The permanent slides were mounted in histological resin for microscopy (Entellan, Merck, Darmstadt, Germany). All immunohistochemical assays included both negative (consisting of reactions omitting the primary antibody) and positive (decidua) controls.[19,20] Images of the immunostained slides were obtained with a Zeiss Axio Scan.Z1 slide scanner (Germany), using a high-power field (HPF = 40x objective),[19,20] to generate digital Tagged Image File Format (TIFF) files.

IGF2 expression in the decidua samples was analyzed blindly using a semiquantitative technique (Allred scoring system),[21] which combines the proportion and intensity of positive immunostained cells. The proportion was calculated as the ratio of positive cells to the total number of cells and was classified as follows: 0 (0%), 1 (>0–1%), 2 (≥1%–10%), 3 (>10%–33%), 4 (>33%–66%), and 5 (>66%–100%). Intensity was classified as 0 (negative), 1+ (weak), 2+ (moderate), and 3+ (strong). The Allred score was calculated by summing the proportion and intensity scores in range from 0 to 8.[21] The mean values of the parameters for the counted fields were used for the statistical analyses. The Zika-infected and uninfected control groups were compared using t test followed by Mann-Whitney U test. Data were analyzed using GraphPad Prism (version 6). Values of $p < 0.05$ indicated significance.

## Results

### RNA-Seq reveals the downregulation of Insulin-like Growth Factor II (*IGF2*) and oxidative phosphorylation pathway dysregulation in naturally infected third trimester human placentas

Six samples of ZIKV-positive and non-ZIKV groups were sequenced. The raw files are available at the NCBI Sequence Read Archive (SRA) (https://www.ncbi.nlm.nih.gov/sra), under the BioProject accession number PRJNA633941.Three samples from each group were selected for differential expression analysis, as follows: LRV/16 931, LRV/16 848, and LRV/16 927 for the ZIKV-positive group, and LRV/16 1387, LRV/16 1094, and LRV/16 1220 for the non-ZIKV group. These samples showed distinct expression patterns visualized by principal component analysis (PCA) and multidimensional scaling plot (MDS) (Fig. S1 and S2; Table S2). Differential gene expression analysis showed 407 genes more expressed in the ZIKV-positive group than in the non-ZIKV group, while 603 genes were downregulated in this comparison (File S1). The hierarchical clustering analysis allowed us to visualize two groups according to ZIKV status (Fig. 1). This list was ordered by the expression measurement and manually inspected.

*IGF2* was identified as differentially expressed according to the ZIKV status with the highest expression level among the downregulated nuclear genes in the ZIKV group (Table 1). RNA-Seq visual inspection showed the splice variants *IGF2-204* (ENST00000381406.8) and *IGF2-205* (ENST00000416167.7) as the two most prevalent *IGF2* transcripts. Further, we sought to determine whether genes encoding *IGF2* protein receptors (*IRS1, IRS2, IGF1R*, and *IGF2R*) or binding proteins (*IGFBP1* to *IGFBP7*, and

Please cite this article as: A.A. Suzukawa, C. Zanluca, N.A.N. Jorge et al., Downregulation of IGF2 expression in third trimester placental tissues from Zika virus infected women in Brazil, Journal of Infection, https://doi.org/10.1016/j.jinf.2020.09.028

**Table 1**
Differential expression analysis according to ZIKV status of *IGF2*, *IGF2*-related nuclear genes, mitochondrial genes, and oxidative phosphorylation nuclear pathway genes.

| | Gene Symbol | logFC | Adjusted *p*-value | DESeq2 base Mean |
|---|---|---|---|---|
| *IGF2* and *IGF2*-related nuclear genes downregulated in ZIKV group | *IGF2* | -1.68 | 0.04 | 6,623 |
| | *IRS1* | -2.46 | < 0.001 | 107 |
| | *IRS2* | -2.66 | 0.002 | 284 |
| | *IGFBP1* | -4.96 | 0.008 | 1,341 |
| | *IGFBP5* | -1.78 | 0.005 | 703 |
| *IGF2*-related nuclear genes upregulated in ZIKV group | *IGF2BP2* | 2.36 | 0.001 | 834 |
| | *IGF2BP3* | 1.87 | 0.01 | 475 |
| IGF binding protein and IGF receptor genes with no differential expression | *IGFBP2* | NSS | 0.30 | 80 |
| | *IGFBP3* | NSS | 0.22 | 923 |
| | *IGFBP4* | NSS | 0.10 | 529 |
| | *IGF1R* | NSS | 0.07 | 546 |
| | *IGF2R* | -1.16 * | < 0.001 | 229 |
| Mitochondrial genes more expressed in ZIKV group | *MT-CO1* | 2.04 | 0.03 | 330,328 |
| | *MT-CO2* | 2.26 | 0.02 | 108,722 |
| | *MT-ND4* | 2.71 | < 0.001 | 102,110 |
| | *MT-ATP6* | 2.63 | 0.04 | 76,250 |
| | *MT-CYB* | 2.59 | 0.003 | 74,181 |
| | *MT-ND5* | 2.60 | < 0.001 | 70,563 |
| | *MT-ND1* | 2.68 | < 0.001 | 51,998 |
| | *MT-ND2* | 3.14 | < 0.001 | 35,307 |
| | *MT-ND4L* | 2.55 | < 0.001 | 15,612 |
| | *MT-ATP8* | 1.99 | 0.02 | 5,204 |
| Oxidative phosphorylation nuclear genes considered together with mitochondrial genes to determine whether pathway is dysregulated | *ATP6V0A1* | -1.57 | < 0.001 | 177 |
| | *SDHA* | -1.70 | 0.03 | 279 |
| | *NDUFB7* | 1.51 | 0.003 | 44 |
| | *TCIRG1* | 0.81 | 0.04 | 307 |
| | *ATP5F1E* | 1.29 | 0.008 | 82 |
| | *COX6B1* | 1.18 | 0.03 | 66 |
| | *COX7C* | 1.10 | 0.03 | 55 |
| | *ATP6V1F* | 1.80 | 0.002 | 60 |
| | *ATP6V1G1* | 1.35 | 0.002 | 163 |
| | *UQCRC2* | -0.99 | 0.01 | 103 |
| | *NDUFB10* | 0.83 | 0.04 | 65 |
| | *ATP6V1C2* | 2.46 | < 0.001 | 650 |
| | *NDUFA6* | 1.19 | 0.02 | 54 |
| | *NDUFA13* | 1.50 | 0.002 | 46 |

NSS: not statistically significant (adjusted p-value > 0.05); *: *IGF2R* presented relative differential expression below the threshold set in this study (|logFC| ≥ 1.5).
Abbreviations: *IRS1*, insulin receptor substrate 1; *IRS2*, insulin receptor substrate 2; *IGFBP1*, insulin like growth factor binding protein 1; *IGFBP5*, insulin like growth factor binding protein 5; *IGF2BP2*, insulin like growth factor 2 mRNA binding protein 2; *IGF2BP3*, insulin like growth factor 2 mRNA binding protein 3; *IGFBP2*, insulin like growth factor binding protein 2; *IGFBP3*, insulin like growth factor binding protein 3; *IGFBP4*, insulin like growth factor binding protein 4; *IGF1R*, insulin like growth factor 1 receptor; *IGF2R*, insulin like growth factor 2 receptor; *MT-CO1*, mitochondrially encoded cytochrome c oxidase I; *MT-CO2*, mitochondrially encoded cytochrome c oxidase II; *MT-ND4*, mitochondrially encoded NADH dehydrogenase 4; *MT-ATP6*, mitochondrially encoded ATP synthase 6; *MT-CYB*, mitochondrially encoded cytochrome b; *MT-ND5*, mitochondrially encoded NADH dehydrogenase 5; *MT-ND1*, mitochondrially encoded NADH dehydrogenase 1; *MT-ND2*, mitochondrially encoded NADH dehydrogenase 2; *MT-ND4L*, mitochondrially encoded NADH 4L dehydrogenase; *MT-ATP8*, mitochondrially encoded ATP synthase 8; *ATP6V0A1*, ATPase H+ transporting V0 subunit a1; *SDHA*, succinate dehydrogenase complex flavoprotein subunit A; *NDUFB7*, NADH,ubiquinone oxidoreductase subunit B7; *TCIRG1*, T cell immune regulator 1, ATPase H+ transporting V0 subunit a3; *ATP5F1E*, ATP synthase F1 subunit epsilon; *COX6B1*, cytochrome c oxidase subunit 6B1; *COX7C*, cytochrome c oxidase subunit 7C; *ATP6V1F*, ATPase H+ transporting V1 subunit F; *ATP6V1G1*, ATPase H+ transporting V1 subunit G1; *UQCRC2*, ubiquinol-cytochrome c reductase core protein 2; *NDUFB10*, NADH,ubiquinone oxidoreductase subunit B10; *ATP6V1C2*, ATPase H+ transporting V1 subunit C2; *NDUFA6*, NADH,ubiquinone oxidoreductase subunit A6; *NDUFA13*, NADH,ubiquinone oxidoreductase subunit A13.

*IGF2BP1* to *IGF2BP3*) were differentially expressed among the samples according to ZIKV status (Table 1). Interestingly, *IRS1, IRS2, IGFBP1*, and *IGFBP5* genes were found to follow the same expression pattern as that of *IGF2*, i.e., downregulated, while *IGF2BP2* and *IGF2BP3* genes were upregulated. However, no differential expression was observed for the *IGF1R, IGF2R, IGFBP2, IGFBP3*, or *IGFBP4* genes. Considering that dysregulation of *IGF2* expression is known to cause impaired fetal development, and that other genes of the IGF system were also modulated in the transcriptome analysis, *IGF2* gene was chosen for experimental validation.

In addition to the IGF2 system genes, RNA-Seq differential expression analysis showed mitochondrial genes (*MT-CO1, MT-CO2, MT-ND4, MT-ATP6, MT-CYB, MT-ND5, MT-ND1, MT-ND2, MT-ND4L*, and *MT-ATP8*) as upregulated in the ZIKV-positive group (Table 1). Gene set enrichment analysis revealed statistically significant dysregulation of the oxidative phosphorylation pathway ($p$-value $< 0.05$), with most of the genes more highly expressed in the ZIKV group. The oxidative phosphorylation was the single pathway identified as statistically significant between ZIKV and non-ZIKV groups.

### *ZIKV infection downregulates* IGF2 *in a cell line model*

To validate the transcriptome results, Caco-2 cells were infected with ZIKV, as these cells express genes in the IGF2 pathway.[22] The infection of Caco-2 cells with the African ZIKV MR766 strain resulted in decreased *IGF2* mRNA levels 48 h.p.i., while the Asian ZIKV ZV BR 2015/15261 isolate did not show a similar level of downregulation until 72 h.p.i. (Fig. 2). Intriguingly, no modulation was observed when the cells were infected with the Asian ZIKV ZV BR 2016/16288 isolate. To investigate whether other flaviviruses modulate *IGF2* expression, Caco-2 cells were infected with either DENV-1, WNV, wild-type (M17/09) YFV or the YFV 17DD vaccine strain. No significant modulation of *IGF2* expression was observed after infection by the abovementioned viruses, except for a mild (<50%) effect observed for 17DD.

To assess whether individual ZIKV fitness differences would impact the *IGF2* gene modulation results, we evaluated the time course of intracellular RNA and E protein synthesis and the secreted virus titers in Caco-2 cells (Fig. 3A-E). Compared to the Asian ZIKV strains, African ZIKV MR766 yielded higher levels of in-

Please cite this article as: A.A. Suzukawa, C. Zanluca, N.A.N. Jorge et al., Downregulation of IGF2 expression in third trimester placental tissues from Zika virus infected women in Brazil, Journal of Infection, https://doi.org/10.1016/j.jinf.2020.09.028

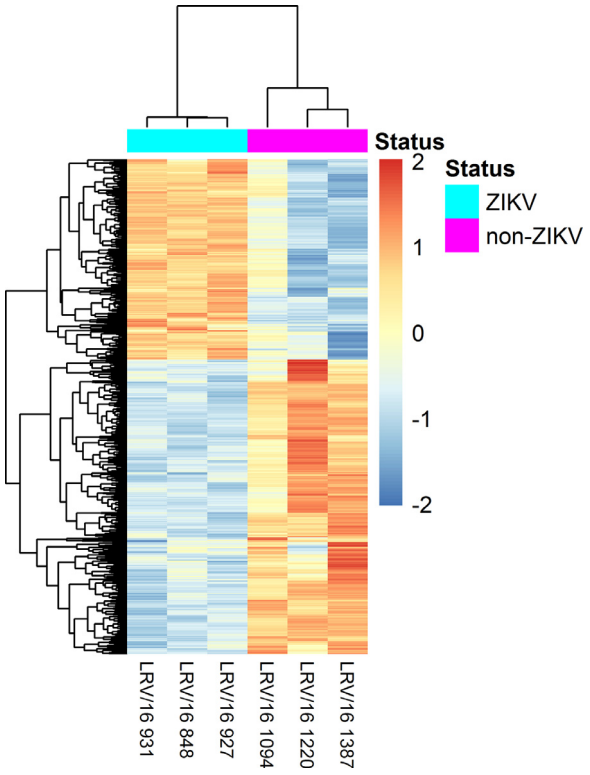


**Fig. 1.** Hierarchical clustering and heat map of $\log_2$-normalized CPM counts of the differentially expressed genes (adjusted $p$-value $\leq 0.05$) of the non-ZIKV and ZIKV samples.

tracellular viral RNA at all time points analyzed (Fig. 3E). Intriguingly, ZIKV ZV BR 2016/16288 isolate infection resulted in a higher number of RNA copies than did infection with the ZIKV ZV BR 2015/15261 isolate 48 h.p.i., with both Asian ZIKV strains showing similar RNA loads 72 h.p.i (Fig. 3E). CT values obtained by real-time RT-PCR targeting viral RNA indicated that all these viruses were able to replicate successfully in this cell model (Table S3). Notably, WNV demonstrated a higher ability to favor RNA synthesis, which resulted in lower CT values, within 24 h.p.i. Similarly, higher RNA levels were obtained for wild-type YFV M17/09 24 h.p.i. than for the vaccine strain, but this difference was reduced at the following time points (Table S3).

Immunofluorescence assays corroborated previously obtained RNA results, since a higher percentage of Caco-2 cells infected by ZIKV MR766, WNV and wild-type YFV M17/09 as early as 24 h.p.i. and peaking 48 h.p.i. (Fig. 3B). WNV and YFV M17/09 sustained high infection levels through 72 h.p.i. On the other hand, the percentage of YFV 17DD-infected cells was higher at 48 h.p.i., while the percentage of DENV-1 E-infected cells increased progressively. Regarding the ZIKV isolates, although ZIKV MR766 infection resulted in a higher percentage of infected cells early, as described above, all three ZIKV isolates had reached similar percentages of infection 48 h.p.i. (Fig. 3B). Then, a decrease was observed for the ZIKV ZV BR 2015/15261 and ZIKV MR766 isolates 72 h.p.i., but not for ZIKV ZV BR 2016/16288. This effect may be related to the different degrees of cytopathic effects induced by the ZIKV ZV BR 2015/15261 and ZIKV MR766 isolates at this time point (Fig. 3A and 3C).

Differences in flavivirus replication in Caco-2 cells were also evaluated by titrating the viral particles released into supernatants over 72 hours. ZIKV MR766 presented with the highest titer levels during all the time points, and no statistical differences were observed between the Asian ZIKV isolates (Fig. 3D). At 72 h.p.i., viral titers in the C6/36 cells ranged from $10^4$ ffu/mL for wild-type YFV M17/09 to $10^7$ ffu/mL for ZIKV MR766 and WNV (Fig. 3D).

### *IGF2 peptide levels are reduced in decidual tissues naturally infected with ZIKV*

Expression of IGF2 was analyzed in the fetal-maternal interface of placental tissues from six naturally ZIKV-infected pregnant women and four non-ZIKV controls. IGF2 was first assessed in the fetal portion of placentas (trophoblast villi), however, no differences were observed (data not shown). Visual inspection indicated a possible role of ZIKV to modulate IGF2 expression in the maternal portion of placentas (decidua), which was chosen for further semiquantitative analysis. Representative images of the deciduae are shown in Fig. 4A. The ratio of the number of IGF2-positive to total cells was reduced in the ZIKV-infected tissues (Fig. 4B and Table S4); these cells also showed significantly lower staining intensity than the negative control samples (Fig. 4C and Table S4). Altogether, the effect of all these parameters resulted in a lower Allred score (Fig. 4D and Table S4), which revealed broad IGF2 downregulation throughout the decidual tissues from women infected by ZIKV at the late stages of pregnancy.

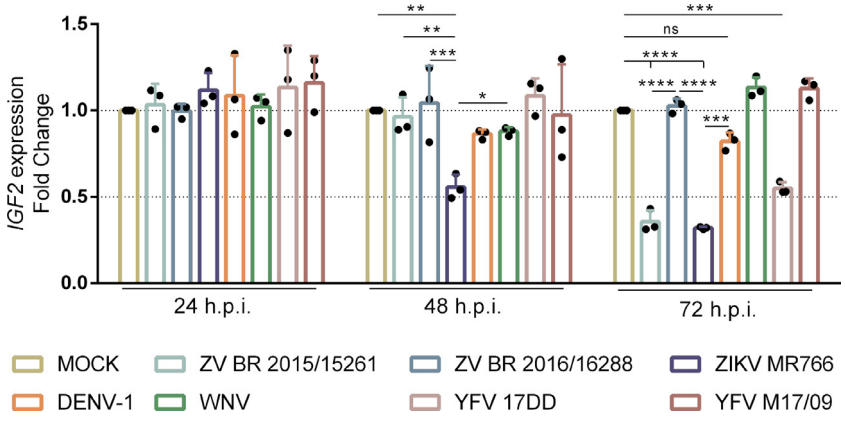


**Fig. 2.** ZIKV downregulates *IGF2* expression in Caco-2 cells. Cells were infected with different flaviviruses, and the gene expression was analyzed 24, 48 and 72 h.p.i. *IGF2* expression was normalized by three endogenous genes (RNase P, SDHA and YWHAZ) according to the $\Delta\Delta$CT method. Data are presented as the means and standard deviation of three independent biological experiments in duplicate. Statistical analysis was performed using two-way ANOVA followed by Tukey's test. ns: not significant; * $p < 0.05$; ** $p < 0.01$; *** $p < 0.001$ and **** $p < 0.0001$.

Please cite this article as: A.A. Suzukawa, C. Zanluca, N.A.N. Jorge et al., Downregulation of IGF2 expression in third trimester placental tissues from Zika virus infected women in Brazil, Journal of Infection, https://doi.org/10.1016/j.jinf.2020.09.028

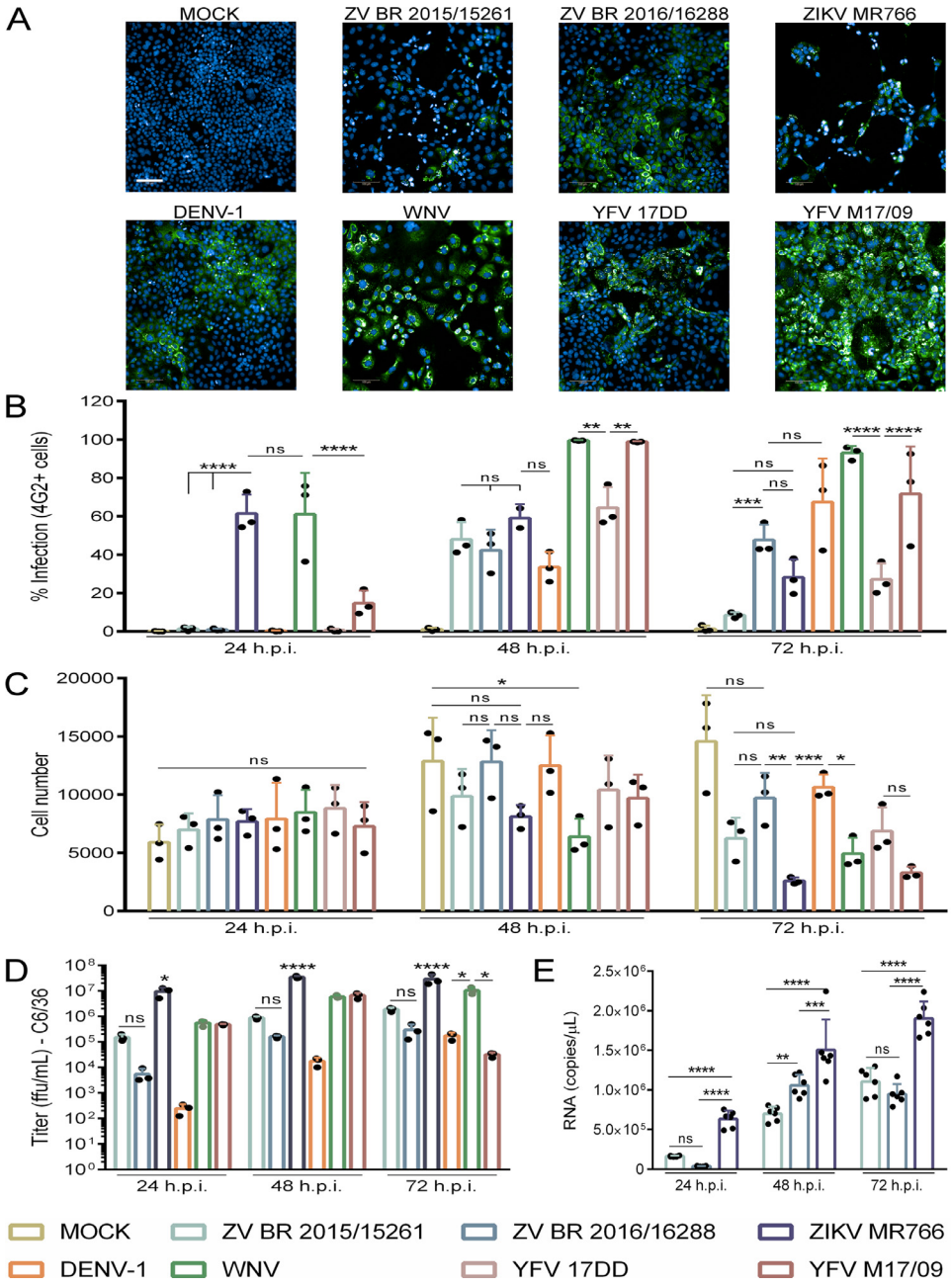


**Fig. 3.** Flavivirus infection in Caco-2 cells. (A) Representative immunofluorescence images of Caco-2 cells infected by different flavivirus 72 h.p.i. Scale bars: 100 µm. (B) Percentage of infected Caco-2 cells was determined according to 4G2 staining of the indicated flaviviruses 24, 48 and 72 h.p.i. Cells were counted with a high content screening imaging system (Operetta). (C) Viral infection leads to time-dependent cell death, as revealed by the progressive reduction in the Caco-2 cell population, depending on the viral isolate. Cell counting was performed by a high content screening imaging system (Operetta) according to number of nuclei stained with a DAPI fluorophore. (D) Supernatants from Caco-2 cell cultures infected with different flaviviruses were titrated 24, 48 and 72 h.p.i. on C6/36 monolayers. (E) Time course of intracellular viral RNA load in Caco-2 cells infected by different ZIKV isolates. Monolayers were washed three times with PBS before the RNA extraction. Viral RNA content was estimated by real-time RT-PCR using a commercial standard curve. The data were analyzed using two-way ANOVA followed by Tukey's multiple comparison test. The graphs are based on the means and standard deviation of three experiments in duplicate. ns: not significant; $^{*}p < 0.05$; $^{**}p < 0.01$; $^{***}p < 0.001$ and $^{****}p < 0.0001$.

## Discussion

Since ZIKV emerged in Brazil, many efforts have been made to understand the mechanisms by which this virus leads to the malformation of fetuses. Detection of the ZIKV genome in amniotic fluid[23,24] and in fetal brain[25,26] indicated that ZIKV crosses the placental barrier and thus might interfere directly with fetal development.

The placenta is the key means of transferring nutrients and oxygen to the fetus and is of particular interest because dysfunctions to it are related to fetal adverse outcomes and disease predisposition.[27] We have previously described the presence of ZIKV RNA and protein in full-term placentas from mothers who were infected in the earliest stages of gestation.[12,28] The persistence of ZIKV in the placenta may have various implications that contribute to adverse fetal outcomes. In addition to this evidence, a unique study explored placental gene modulation in humans after ZIKV infection to reveal transcriptional differences in eIF2 signaling and mitochondrion and oxidative phosphorylation-related genes.[29] Notably, these data were obtained from a single case of a woman infected

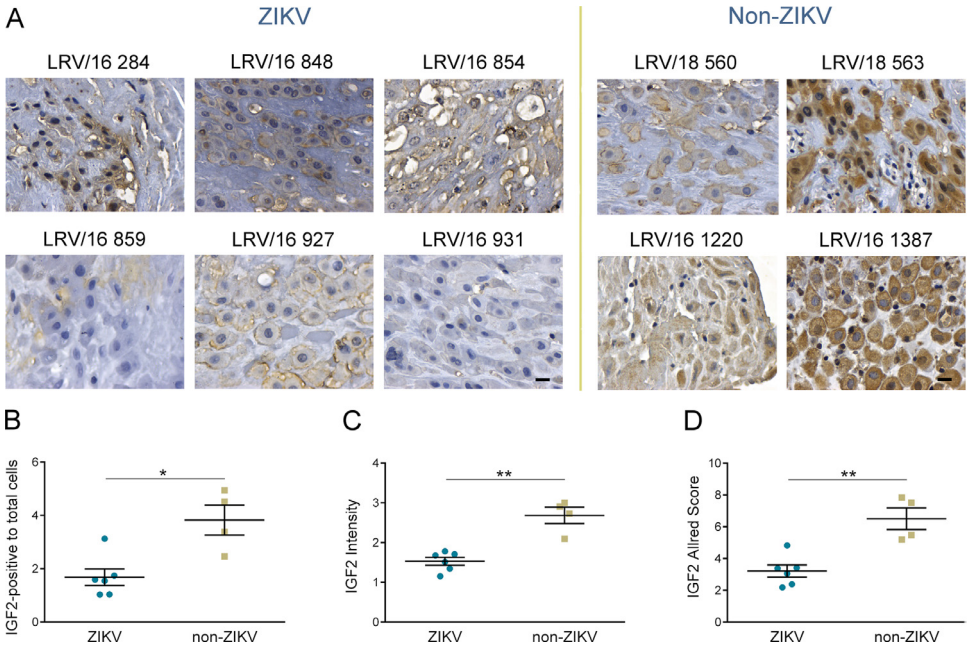


**Fig. 4.** Illustrative panel depicting immunohistochemical targeting IGF2 in third-trimester human deciduae is shown in (A). The tissues were blindly analyzed and scored as detailed in the Material and Methods. Scale bars: 20 µm. IGF2-positive to total cells (proportion) (B) and intensity (C) of ZIKV-positive and ZIKV-negative deciduae. These variables were combined and expressed in the Allred scoring (D). Statistical analysis was performed using the t test followed by the Mann-Whitney U test. Data represent mean ± SD. $^{*}p < 0.05$; $^{**}p < 0.01$.

during the first trimester of pregnancy, and the possibility cannot be excluded that other affected pathways were not detected during the time that elapsed between the time of infection and the delivery, when the tissues were obtained. Furthermore, individual intrinsic genetic heterogeneity must be considered.

Here, we investigated genes differentially expressed in placental tissues from naturally infected women that might disturb the delicate interplay between the mother and fetus interface. The transcriptome data obtained from the placental tissues of three women infected with ZIKV during the third trimester of gestation were compared to those from three non-ZIKV women. The rationale for using samples from women who were infected during the late stages of pregnancy was based on the objective to have the timing of virologic and immunological analyses as close as possible to the emergence of acute ZIKV infection.

In our study, the three samples in each group exhibited gene expression pattern clustering, as indicated using PCA and MDS. According to Zika status, 1010 differentially expressed genes were identified. Interestingly, *IGF2* gene was consistently downregulated in ZIKV positive samples, with expression that was -1.68-fold lower in the ZIKV-positive samples than it was in the controls (Table 1).

IGF2 is a protein hormone that participates in the insulin/insulin-like growth factor system. The IGF axis controls fetal growth during pregnancy through the combination of IGF1, IGF2, IGF receptors, insulin receptors, IGF binding proteins, and protein phosphorylation (reviewed by Forbes and Westwood[30]). During pregnancy, IGF2 is synthesized by placental and fetal tissues and, through paracrine, autocrine and endocrine effects, is involved in the regulation of both fetal and placental development.[10,11] IGF2 also regulates the proliferation and apoptosis of first-trimester extravillous cytotrophoblasts *in vitro*, and it is speculated that this mechanism could be relevant to embryo implantation[31] The expression of *IGF2* is controlled by genomic imprinting; fetal growth disorders, such as Beckwith-Wiedemann syndrome, result from dysregulation of the IGF2 balance.[32] Studies using murine models demonstrated that IGF2 is also important to adult[33] as well as fetal neurogenesis, a concept supported by the fact that knocking out the *IGF2* gene resulted in decreased fetal brain weight.[34] According to our analysis, in addition to the reduced expression of *IGF2* in the ZIKV placentas, we identified other downregulated (*IGFBP1, IGPBP5, IRS1*, and *IRS2*) as well as upregulated (*IGF2BP2* and *IGF2BP3*) genes of the IGF system, reinforcing the hypothesis that this system is dysregulated after ZIKV infection.

Evidence indicating that ZIKV may interfere with IGF pathway gene expression has been described recently by Glover and colleagues[35] that showed activation of IGF1 pathway signaling in Vero cells after ZIKV infection. Primary human astrocytes infected with either African and Asian ZIKV strains secreted less IGF2 than levels secreted by the controls.[36] However, in both studies, these findings were not further explored by the authors. Recent data from Karuppan and colleagues[37] demonstrated a significant reduction in IGF1 expression in the brains of pups from ZIKV-infected Beclin-1-deficient mouse dams. It was speculated that the downregulation of this protein potentially contributed to the smaller and underdeveloped brain of pups in the litter.

Attempts to validate our RNA-Seq results using real-time RT-PCR of the RNA extracted from nonfixed placentas were unsuccessful, likely due to the random method of placental sampling that was utilized. It is known that *IGF2* mRNA distribution varies throughout the placenta according to pregnancy gestational age.[38] Tissues were obtained at delivery time in different hospitals in that State of Paraná during a Zika outbreak in Brazil, and unfortunately, no dissection was performed before the tissues were frozen, which made it impossible to separate the maternal (decidua) from the fetal part of the placentas. This issue would potentially yield biased results. An additional limitation was reliance on the choice of an endogenous normalizer gene, since the most stable genes may vary according to fetal sex and clinical conditions.[39–41] Nevertheless, because of the abovementioned restrictions, we used a cell culture model to validate the RNA-Seq results.

Caco-2 cells were chosen for *IGF2* data validation because according to the Human Protein Atlas database,[42] Caco-2 cells shows the highest *IGF2* gene expression levels among various human

cells lines, which was essential to test the modulation of IGF2 transcription during ZIKV and other flaviviruses infection. Of note, placental-derived lineages, such as BeWo, do not express *IGF2*[42]. We found that Caco-2 cells were permissive to all the flaviviruses used in this study, as revealed by intracellular RNA (Table S3), E protein synthesis (Fig. 3B) and viral release (Fig. 3D). *IGF2* gene expression in the ZIKV-infected Caco-2 cells, as measured by real-time RT-PCR, supported the RNA-Seq data. *IGF2* was downregulated due to infection by both Asian and African ZIKV strains in a time-dependent manner. A 3-fold reduction in *IGF2* expression was found in Caco-2 cells 72 hours after ZIKV MR766 or ZIKV ZV BR 2015/15261 infection (Fig. 2). The downregulation of *IGF2* gene expression occurred earlier for ZIKV MR766 than it was for ZIKV ZV BR 2015/15261, since a reduction of nearly 50% was detected 48 h.p.i. for the African strain (Fig. 2). This result may be due to the high viral fitness of ZIKV MR766 compared to the other ZIKV low passaged recent clinical isolates, as revealed by the presence of the higher levels of intracellular viral RNA content within 24 h.p.i. (Fig. 3E), higher viral titers (Fig. 3D) and the higher percentage of infected cells observed at the same time point (Fig. 3B). Notably, ZIKV MR766 is a laboratory-adapted strain, while the Asian isolates used in this study were recently obtained from Brazilian clinical samples not extensively passaged.[15] Remarkably, differences in the ability to downregulate IGF2 between the two recently obtained low-passage clinical Asian ZIKV isolates (ZV BR 2015/15261 and ZV BR 2016/16288) were observed. This finding was intriguing since similar RNA and percentages of cells expressing E protein were observed for both isolates (Fig. 3B and 3E), although ZIKV ZV BR 2016/16288 infection was found to result in a slightly lower viral titer (Fig. 3D). Importantly, both ZIKV ZV BR 2016/16288 and ZV BR 2015/15261 were isolated from patients exhibiting similar clinical symptoms in southern Brazil in January 2016 and northeast Brazil in June 2015,[15] respectively. Studies on the effects of ZIKV on human astrocytes have also observed similar profiles among samples, with lower IGF2 release found after astrocyte infection with ZIKV MR766 or Asian PRVABC59 Puerto Rico ZIKV strains but not with the Honduras ZIKV R103451 strain.[36] The mechanisms involved in the regulation of *IGF2* gene expression by ZIKV need to be further investigated, but our results indicate the possible involvement of six amino acid differences found between the recent ZIKV clinical isolates ZV BR 2016/16288 and ZV BR 2015/15261 that map to NS1, NS2A, NS3 and NS4B proteins.[15]

IGF2 expression modulation has been described for other viruses. Dysregulation of the IGF system by human papillomavirus (HPV), hepatitis B virus (HBV) and hepatitis C virus (HCV) is associated with disease progression and cancer development. In HBV and HCV-related hepatocarcinogenesis, IGF2 expression is augmented.[43–45] HPV 16 infection downregulates IGF-binding protein 2 (IGFBP2) expression, leading to an increase in IGF1 and IGF2 signaling and consequently to increasing cell invasion and disease severity.[46]

Although the epidemiological data are still controversial,[47,48] mouse models have indicated that West Nile infection during pregnancy may result in birth defects.[49] We also sought to determine whether WNV and other flaviviruses can disturb *IGF2* gene expression. To make this determination, Caco-2 cells were infected with DENV-1, WNV and both the vaccine form and wild-type YFV. Interestingly, no significant differences in *IGF2* expression were found for DENV-1, WNV or wild-type YFV when compared to the mock-infected controls at any of the time points analyzed (Fig. 2). Apparently, the difference in results for ZIKV and the other viruses was not related solely to replication ability, since DENV-1 RNA, percentage of infected cells and viral titers were similar to those found for ZIKV ZV BR 2015/15261, while the WNV and wild-type YFV replication kinetics were comparable to those of ZIKV MR766, although ZIKV MR766 had the highest viral titers (Fig. 3A-C). In addition to ZIKV, in our cell culture model, only the YFV 17DD vaccine induced downregulation of *IGF2* (Fig. 2); this result also seems to be related to factors other than virus replication itself, since wild-type YFV presented with higher viral fitness than did 17DD YFV (Fig. 3B and Table S3). Clinical data concerning adverse events resulting from the unintentional 17DD YFV vaccination of pregnant women are not completely conclusive,[50] and other factors, such as the ability of the virus to cross the placental barrier, must be considered when analyzing the biological relevance of the results obtained from *in vitro* models.

Immunohistochemical analysis of naturally infected ZIKV decidual tissues obtained at delivery from women who had been infected at late gestation stages showed reduced IGF2 staining in both proportion and intensity (Fig. 4B and 4C). This IGF2 differential modulation seems to be more related to the deciduae than to trophoblasts, since no significant differences in IGF2 staining were observed for the trophoblasts (data not shown).

Deletion of the transcript of *IGF2* in the placentas of mice (*Igf2P0*) disturbed the ability of the placentas to adapt to protein undernutrition, which resulted in a low-weight pups.[51] Recently, protein malnutrition has been implicated in the worst fetal outcomes for mice infected with ZIKV.[52] This malnutrition and infection combination also resulted in impairment to the placental structure and in reduced body growth and neuronal development of the pups compared to the growth and development of pups born to dams that received a standard diet. Unfortunately, no information on the development of the babies born to the women participating in this study was available to investigate the relationship between nutritional status, individual IGF2 levels and pregnancy outcomes. Nevertheless, the mechanisms affecting the relationship between ZIKV infection, placental function and fetal outcomes are being gradually revealed, making it possible to understand the reasons why not every ZIKV infection during pregnancy results in congenital disease.[53] Furthermore, additional processes may also be involved in ZIKV pathogenesis, such as mitochondrial and oxidative phosphorylation gene dysregulation (Table 1). This dysregulation has been previously observed during placental transcriptome profiling[29] and may be related to an overall cellular energy imbalance induced by ZIKV infection.[54]

In summary, we conclude that ZIKV differs from other flaviviruses in downregulating *IGF2* gene expression, although further studies are necessary to investigate the mechanisms involved. We also showed that mutations in the ZIKV genome may result in differences in the biology of the viruses and, consequently, the host response. Although other factors, such as maternal nutrition or drug and alcohol consumption, may contribute to the fetal outcome of mothers infected with ZIKV during pregnancy, our findings focused to the role of placental factors, especially IGF2, that can contribute to Zika congenital syndrome in humans and can open avenues to the development of therapies to mitigate ZIKV-induced fetal injuries.

## Author contributions

AAS, CZ, LN, MMD, CMR and CNDS contributed to the study design; FP, NANJ, AFFHF and VSCP performed the RNA-Seq data analysis; AAS, CZ, ACK and JB performed the cell culture experiments; CBVP performed the IHC assays; SG performed the image analysis; LN and PZR analyzed the tissue slides and performed the Allred semiquantitative analysis; AAS,CZ, FP, LN, ACK, MRM, CMR and CNDS analyzed the overall results; AAS,CZ, FP, LN, ACK, JB and CNDS wrote the manuscript.

## Declaration of Competing Interest

The authors have declared that no conflict of interest exists.

Please cite this article as: A.A. Suzukawa, C. Zanluca, N.A.N. Jorge et al., Downregulation of IGF2 expression in third trimester placental tissues from Zika virus infected women in Brazil, Journal of Infection, https://doi.org/10.1016/j.jinf.2020.09.028

## Acknowledgments

The authors are grateful to Dr. Érico Tosoni Costa for kindly providing us with Caco-2 cells, Dr. Edna Teruko Kimura for donating anti-IGF2 antibody, Luana Ebbinghaus for technical support, Dr. Thiago Jacomasso for helping with the PCR gene expression data analysis and Dr. Hellen Geremias dos Santos for assistance using R. They are also grateful to Connie Zhao from the Rockefeller University Genomics Resource Center for support in sequencing and to Wagner Nagib for graphical design.

## Funding

This work was supported by CNPq (Conselho Nacional de Desenvolvimento Científico e Tecnológico, Brazil) [grant number 439968/2016-0], Fiocruz (Fundação Oswaldo Cruz), and Inova Fiocruz/VPPCB [grant number VPPCB-007-FIO-18-2-19]. CNDS, LN, FP and JB received a CNPq fellowship. This study was financed in part by the Coordenação de Aperfeiçoamento de Pessoal de Nível Superior – Brasil (CAPES) [grant number 88887.124207/2016-00] and Finance Code 001 (M.Sc. scholarship to VSCP and AFFHF). The work was also supported in part through anonymous donors to a Rockefeller University Zika virus research fund.

## Supplementary materials

Supplementary material associated with this article can be found, in the online version, at doi:10.1016/j.jinf.2020.09.028.

## References

1. Duffy Mark R, Ho Chen Tai, Thane Hancock W, Powers Ann M, Kool Jacob L, Lanciotti Robert S. et al. Zika virus outbreak on Yap Island, Federated states of micronesia. *N Engl J Med* 2009;**360**(24):2536–43. doi:10.1056/NEJMoa0805715.
2. Zanluca Camila, De Melo Vanessa Campos Andrade, Mosimann Ana Luiza Pamplona, Dos Santos Glauco Igor Viana, dos Santos Claudia Nunes Duarte, Luz Kleber. First report of autochthonous transmission of Zika virus in Brazil. *Mem Inst Oswaldo Cruz* 2015;**110**(4):569–72. doi:10.1590/0074-02760150192.
3. Brasil P, Pereira JP, Moreira ME, MRibeiro Nogueira R, Damasceno L, Wakimoto M, et al. Zika virus infection in pregnant women in Rio de Janeiro. *N Engl J Med* 2016;**375**(24):2321–34. doi:10.1056/NEJMoa1602412.
4. Martines Roosecelis Brasil, Bhatnagar Julu, de Oliveira Ramos Ana Maria, Davi Helaine Pompeia Freire, Iglezias Silvia DAndretta, Kanamura Cristina Takami, et al. Pathology of congenital Zika syndrome in Brazil: a case series. *Lancet* 2016;**388**(10047):898–904. doi:10.1016/S0140-6736(16)30883-2.
5. Rice Marion E, Galang Romeo R, Roth Nicole M, Ellington Sascha R. Vital signs : Zika-associated birth defects and neurodevelopmental abnormalities possibly associated with congenital Zika Virus infection —. *Morb Mortal Wkly Rep, CDC* 2018;**67**(31):858–67.
6. Svetlana Khaiboullina, Timsy Uppal, Konstatin Kletenkov, St Jeor Stephen Charles, Ekaterina Garanina, Albert Rizvanov, et al. Transcriptome profiling reveals pro-inflammatory cytokines and matrix metalloproteinase activation in Zika virus infected human umbilical vein endothelial cells. *Front Pharmacol* 2019;**10**(642):1–17. doi:10.3389/fphar.2019.00642.
7. Kant Tiwari Shashi, Jason Dang, Yue Qin, Gianluigi Lichinchi, Vikas Bansal, Rana Tariq M. Zika virus infection reprograms global transcription of host cells to allow sustained infection. *Emerg Microbes Infect* 2017;**6**(4) e24-10. doi:10.1038/emi.2017.9.
8. Lima Morganna C, de Mendonça Leila, Rezende Antonio R, Carrera Raquel M, Aníbal-Silva Conceição M, Demers Matthew E, et al. The transcriptional and protein profile from human infected neuroprogenitor cells is strongly correlated to zika virus microcephaly cytokines phenotype evidencing a persistent inflammation in the CNS. *Front Immunol* 2019;**10**(1928). doi:10.3389/fimmu.2019.01928.
9. Kumar Singh Pawan, Indu Khatri, Alokkumar Jha, Pretto Carla D, Spindler Katherine R, Arumugaswami Vaithilingaraja, et al. Determination of system level alterations in host transcriptome due to Zika virus (ZIKV) Infection in retinal pigment epithelium. *Sci Rep* 2018;**8**(1):1–16. doi:10.1038/s41598-018-29329-2.
10. Ursula Hiden, Elisabeth Glitzner, Michaele Hartmann, Gernot Desoye. Insulin and the IGF system in the human placenta of normal and diabetic pregnancies. *J Anat* 2009;**215**(1):60–8. doi:10.1111/j.1469-7580.2008.01035.x.
11. Daniel Bergman, Matilda Halje, Matilda Nordin, Wilhelm Engström. Insulin-like growth factor 2 in development and disease: a mini-review. *Gerontology* 2013;**59**(3):240–9. doi:10.1159/000343995.
12. Lucia Noronha, Camila Zanluca, Marion Burger, Akemi Suzukawa Andreia, Marina Azevedo, Rebutini Patricia Z, et al. Zika virus infection at different pregnancy stages: Anatomopathological findings, target cells and viral persistence in placental tissues. *Front Microbiol* 2018;**9**(2266):1–11. doi:10.3389/fmicb.2018.02266.
13. Weijun Luo, Friedman Michael S, Kerby Shedden, Hankenson Kurt D, Woolf Peter J. GAGE: Generally applicable gene set enrichment for pathway analysis. *BMC Bioinformatics* 2009;**10**:1–17. doi:10.1186/1471-2105-10-161.
14. Weijun Luo, Cory Brouwer. Pathview: an R/Bioconductor package for pathway-based data integration and visualization. *Bioinformatics* 2013;**29**(14):1830–1. doi:10.1093/bioinformatics/btt285.
15. Maria Strottmann Daisy, Camila Zanluca, Pamplona Mosimann Ana Luiza, Koishi Andrea C, Auwerter Nathalia Cavalheiro, Faoro Helisson, et al. Genetic and biological characterization of zika virus isolates from different Brazilian regions. *Mem Inst Oswaldo Cruz* 2019;**114**(7):1–11. doi:10.1590/0074-02760190150.
16. Ricciardi Jorge Taissa, Pamplona Mosimann Ana Luiza, Lucia de Noronha, Angela Maron, Nunes Duarte dos Santos Claudia. Isolation and characterization of a Brazilian strain of yellow fever virus from an epizootic outbreak in 2009. *Acta Trop* 2017;**166**:114–20. doi:10.1016/j.actatropica.2016.09.030.
17. Livak Kenneth J, Schmittgen Thomas D. Analysis of relative gene expression data using real-time quantitative PCR and the 2-ΔΔCT method. *Methods* 2001;**25**(4):402–8. doi:10.1006/meth.2001.1262.
18. Cristine Koishi Andrea, Akemi Suzukawa Andréia, Camila Zanluca, Elena Camacho Daria, Guillermo Comach, Nunes Duarte dos Santos Claudia. Development and evaluation of a novel high-throughput image-based fluorescent neutralization test for detection of Zika virus infection. *PLoS Negl Trop Dis* 2018;**12**(3):1–15. doi:10.1371/journal.pntd.0006342.
19. Paula Percicote Ana, Lazaretti Mardegan Gabriel, Schneider Gugelmim Elizabeth, Ossamu Ioshii Sergio, Paula Kuczynski Ana, Seigo Nagashima, et al. Tissue expression of retinoic acid receptor alpha and CRABP2 in metastatic nephroblastomas. *Diagn Pathol* 2018;**13**(1):1–7. doi:10.1186/s13000-018-0686-z.
20. Adalgisa Simões Mona, Cesar Pabis Francisco, Ehrenfried de Freitas Ana Karyn, Viola de Azevedo Marina Luise, Martins Ronchi Daiane Cristine, Lucia de Noronha. Immunoexpression of GADD45$\beta$ in the myocardium of newborns experiencing perinatal hypoxia. *Pathol Res Pract* 2017;**213**(3):222–6. doi:10.1016/j.prp.2016.12.011.
21. Harvey Jennet M, Clark Gary M, Kent Osborne C, Craig Allred D. Estrogen receptor status by immunohistochemistry is superior to the Ligand-Binding assay for predicting response to Adjuvant Endocrine therapy in breast cancer. *J Clin Oncol* 1999;**17**(5):1474–81.
22. Andreas Hoeflich, Yi Yang, Ulrike Kessler, Peter Heinz-Erian, Helmut Kolb, Wieland Kiess. Human colon carcinoma cells ( CaCo-2) synthesize IGF-II and express IGF-I receptors and IGF-II/M6P receptors. *Mol Cell Endocrinol* 1994;**101**(1–2):141–50. doi:10.1016/0303-7207(94)90228-3.
23. Marcela Mercado, Ailes Elizabeth C, Marcela Daza, Tong Van T, Osorio Johana, Valencia Diana, et al. Zika virus detection in amniotic fluid and Zika-associated birth defects. *Am J Obstet Gynecol* 2020;**222**(6) 610.e1-610.e13. doi:10.1016/j.ajog.2020.01.009.
24. Guilherme Calvet, Aguiar Renato S, Melo Adriana SO, Sampaio Simone A, de Filippis Ivano, Fabri Allison, et al. Detection and sequencing of Zika virus from amniotic fluid of fetuses with microcephaly in Brazil: a case study. *Lancet Infect Dis* 2016;**16**(6):653–60. doi:10.1016/S1473-3099(16)00095-5.
25. Lucia Noronha, Camila Zanluca, Viola Azevedo Marina Luize, Luz Kleber Giovanni, dos Santos Claudia Nunes Duarte. Zika virus damages the human placental barrier and presents marked fetal neurotropism. *Mem Inst Oswaldo Cruz* 2016;**111**(5):287–93. doi:10.1590/0074-02760160085.
26. Brasil Martines Roosecelis, Julu Bhatnagar, Kelly Keating M, Luciana Silva-flannery, Joy Gary, Cynthia Goldsmith, et al. Evidence of Zika virus infection in brain and placental tissues from two congenitally infected newborns and two fetal losses - Brazil, 2015. *Morb Mortal Wkly Rep* 2016;**65**(6):2015–16.
27. Longtine MS, Nelson DM. Placental Dysfunction and fetal programming: the importance of placental size, shape, histopatology, and molecular composition. *Semin Reprod Medeical J* 2013;**29**(3):187–96. doi:10.1055/s-0031-1275515.Placental.
28. Rosenberg Avi Z, Yu Weiying, Ashley Hill D, Reyes Christine A, Schwartz David A. Placental pathology of zika virus: Viral infection of the placenta induces villous stromal macrophage (Hofbauer Cell) proliferation and hyperplasia. *Arch Pathol Lab Med* 2017;**141**(1):43–8. doi:10.5858/arpa.2016-0401-OA.
29. Moon Lum Fok, Vipin Narang, Susan Hue, Jie Chen, Naomi McGovern, Ravisankar Rajarethinam, et al. Immunological observations and transcriptomic analysis of trimester-specific full-term placentas from three Zika virus-infected women. *Clin Transl Immunol* 2019;**8**(11):1–15. doi:10.1002/cti2.1082.
30. Karen Forbes, Melissa Westwood. The IGF axis and placental function: a mini review. *Horm Res* 2008;**69**(3):129–37. doi:10.1159/000112585.
31. Huiyue Chen, Yating Li, Jia Shi, Weiwei Song. Role and mechanism of insulin-like growth factor 2 on the proliferation of human trophoblasts in vitro. *J Obstet Gynaecol Res* 2016;**42**(1):44–51. doi:10.1111/jog.12853.
32. Adele Murrell, Sarah Heeson, Cooper Wendy N, Douglas Eleanor, Apostolidou Sophia, Moore Gudrun E, et al. An association between variants in the IGF2 gene and Beckwith-Wiedemann syndrome: Interaction between genotype and epigenotype. *Hum Mol Genet* 2004;**13**(2):247–55. doi:10.1093/hmg/ddh013.
33. Oliver Bracko, Tatjana Singer, Stefan Aigner, Marlen Knobloch, Beate Winner, Jasodhara Ray, et al. Gene expression profiling of neural stem cells and their neuronal progeny reveals IGF2 as a regulator of adult hippocampal neurogenesis. *J Neurosci* 2012;**32**(10):3376–87. doi:10.1523/JNEUROSCI.4248-11.2012.
34. John O'Kusky, Ping Ye. Neurodevelopmental effects of insulin-like growth factor signaling. *Front Neuroendocrinol* 2012;**33**(3):230–51. doi:10.1016/j.yfrne.2012.06.002.

35. Glover Kathleen KM, Ang Gao, Ali Zahedi-Amiri, Coombs Kevin M. Vero Cell proteomic changes induced by Zika virus infection. *Proteomics* 2019;**19**(4):e1800309. doi:10.1002/pmic.201800309.
36. Raj Ojha Chet, Myosotys Rodriguez, Muthu Karuppan Mohan Kumar, Jessica Lapierre, Fatah Kashanchi, Nazira El-Hage. Toll-like receptor 3 regulates Zika virus infection and associated host inflammatory response in primary human astrocytes. *PLoS One* 2019;**14**(2):1–26. doi:10.1371/journal.pone.0208543.
37. Muthu Karuppan Mohan Kumar, Raj Ojha Chet, Myosotys Rodriguez, Jessica Lapierre, Javad Aman M, Fatah Kashanchi, et al. Reduced-Beclin1-expressing Mice Infected with Zika-R103451 and viral-associated pathology during pregnancy. *Viruses* 2020;**12**(6):608. doi:10.3390/v12060608.
38. Han V K, Bassett N, Walton J, Challis J R. The expression of insulin-like growth factor (IGF) and IGF-binding protein (IGFBP) genes in the human placenta and membranes: evidence for IGF-IGFBP interactions at the feto-maternal interface. *J Clin Endocrinol Metab* 1996;**81**(7):2680–93. doi:10.1210/jcem.81.7.8675597.
39. Drewlo S, Levytska K, Kingdom J. Revisiting the housekeeping genes of human placental development and insufficiency syndromes. *Placenta* 2012;**33**(11):952–4. doi:10.1016/j.placenta.2012.09.007.
40. Cleal JK, Day PL, Hanson MA, Lewis RM. Sex differences in the mRNA levels of housekeeping genes in human Placenta. *Placenta* 2010;**31**:556–7. doi:10.1016/j.placenta.2010.03.006.
41. Yanli Li, Huifang Lu, Yizhen Ji, Sufang Wu, Yongbin Yang. Identification of genes for normalization of real-time RT-PCR data in placental tissues from intrahepatic cholestasis of pregnancy. *Placenta* 2016;**48**:133–5. doi:10.1016/j.placenta.2016.10.017.
42. Mathias Uhlen, Cheng Zhang, Sunjae Lee, Evelina Sjöstedt, Linn Fagerberg, Gholamreza Bidkhori, et al. A pathology atlas of the human cancer transcriptome. *Science (80- )* 2017;**357**(6352):eaan2507. doi:10.1126/science.aan2507.
43. Aldona Kasprzak, Agnieszka Adamek. The insulin-like growth factor (IGF) signaling axis and hepatitis C virus-associated carcinogenesis (Review). *Int J Oncol* 2012;**41**(6):1919–31. doi:10.3892/ijo.2012.1666.
44. Lin Ha Hye, Taeho Kwon, Seon Bak In, Erikson Raymond L. Kim Bo Yeon, Yu Dae Yeul. IGF-II induced by hepatitis B virus X protein regulates EMT via SUMO mediated loss of E- cadherin in mice. *Oncotarget* 2016;**7**(35):56944–57. doi:10.18632/oncotarget.10922.
45. Yuanyuan Ji, Zhidong Wang, Haiyan Chen, Lei Zhang, Fei Zhuo, Qingqing Yang. Serum from Chronic Hepatitis B Patients promotes growth and proliferation via the IGF-II/IGF-IR/MEK/ERK Signaling Pathway in Hepatocellular Carcinoma Cells. *Cell Physiol Biochem* 2018;**47**(1):39–53. doi:10.1159/000489744.
46. Adam Pickard, McDade Simon S, McFarland Marie, McCluggage WGlenn, Wheeler Cosette M, McCance Dennis J. HPV16 Down-regulates the insulin-like growth factor binding Protein 2 to promote Epithelial Invasion in organotypic cultures. *PLoS Pathog* 2015;**11**(6):1–23. doi:10.1371/journal.ppat.1004988.
47. O'Leary Daniel R, Stephanie Kuhn, Kniss Krista L, Hinckley Alison F, Rasmussen Sonja A, John Pape W, et al. Birth outcomes following west nile virus infection of pregnant women in the United States: 2003-2004. *Pediatrics* 2006;**117**(3):2003–4. doi:10.1542/peds.2005-2024.
48. Gabriella Pridjian, Sirois Patricia A, McRae Scott, Hinckley Alison F, Rasmussen Sonja A, Kissinger Patricia, et al. Prospective study of pregnancy and newborn outcomes in mothers with West nile illness during pregnancy. *Birth Defects Res Part A - Clin Mol Teratol* 2016;**106**(8):716–23. doi:10.1002/bdra.23523.
49. Platt Derek J, Smith Amber M, Nitin Arora, Diamond Michael S, Coyne Carolyn B, Miner Jonathan J. Zika virus-related neurotropic flaviviruses infect human placental explants and cause fetal demise in mice. *Sci Transl Med* 2018;**10**(426):1–11. doi:10.1126/scitranslmed.aao7090.
50. Ruben Porudominsky, Gotuzzo Eduardo H. Yellow fever vaccine and risk of developing serious adverse events: a systematic review. *Rev Panam Salud Pública* 2018;**42**. doi:10.26633/RPSP.2018.75.
51. Sferruzzi-Perri Amanda N, Vaughan OR, Coan PM, Suciu MC, Darbyshire R, Constancia M, et al. Placental-specific Igf2 deficiency alters developmental adaptations to undernutrition in mice. *Endocrinology* 2011;**152**(8):3202–12. doi:10.1210/en.2011-0240.
52. Barbeito-Andrés J, Pezzuto P, Higa LM, Dias AA, Vasconcelos JM, Santos TMP, et al. Congenital Zika syndrome is associated with maternal protein malnutrition. *Sci Adv* 2020;**6**(2):eaaw6284. doi:10.1126/sciadv.aaw6284.
53. Bruno Hoen, Bruno Schaub, Funk Anna L, Vanessa Ardillon, Manon Boullard, André Cabié, et al. Pregnancy outcomes after ZIKV infection in French territories in the Americas. *N Engl J Med* 2018;**378**(11):985–94. doi:10.1056/NEJMoa1709481.
54. Flores Ledur Pítia, Karina Karmirian, da Silva Gouveia Pedrosa Carolina, Quintino Souza Leticia Rocha, Gabriela Assis-de-Lemos, Martino Martins Thiago, et al. Zika virus infection leads to mitochondrial failure, oxidative stress and DNA damage in human iPSC-derived astrocytes. *Sci Rep* 2020;**10**(1):1–14. doi:10.1038/s41598-020-57914-x.

Please cite this article as: A.A. Suzukawa, C. Zanluca, N.A.N. Jorge et al., Downregulation of IGF2 expression in third trimester placental tissues from Zika virus infected women in Brazil, Journal of Infection, https://doi.org/10.1016/j.jinf.2020.09.028